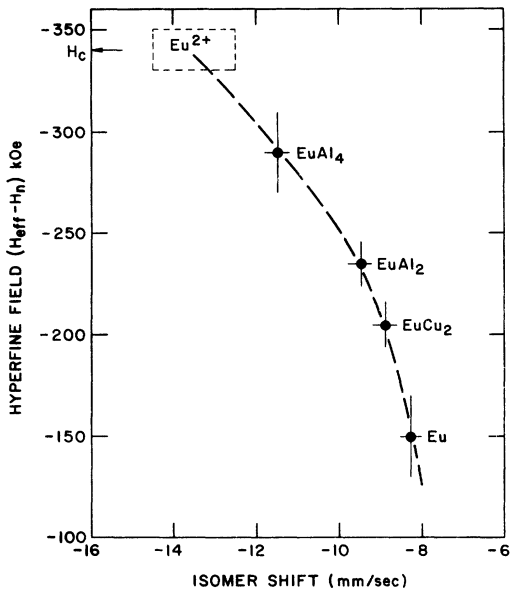

FIG. 3. Correlation between the isomer shift and the single-ion contribution to the hyperfine field, $H_{\text{core}}+H_{\text{op}}$. All isomer shift values are relative to ^{151}Eu in Sm_2O_3.

measure the same quantities. H_c+H_{op} is proportional to the spin density at the nucleus and the isomer shift is proportional to the charge density at the nucleus. However, if the polarizability of s electrons does not vary substantially in these various materials, a correlation such as observed may be expected. One may also notice from Table I that the isomer shift is independent of concentration in a given alloy system. That fact, coupled with the correlation of Fig. 3, provides experimental evidence for the previous assumption that H_{op} is independent of concentration.

(iii) The hyperfine field of $(Eu^{2+})La^{3+}Al_2$ is -205 kOe. From Ref. 6 one finds a value of -140 kOe for $(Gd^{3+})Y^{3+}Al_2$. The difference may be easily understood as a repulsion of conduction electrons by the divalent Eu ion in the trivalent matrix. Thus H_{op} is decreased by 65 kOe.

(iv) The hyperfine field of $(Eu^{2+})Yb^{2+}Al_2$ is -235 kOe, as compared with the value[6] of -140 kOe for $(Gd^{3+})Y^{3+}Al_2$. Here the difference cannot be due to the charge screening effect just mentioned. Instead it is most likely due to an increase of 95 kOe in H_{op} due to the additional conduction electron available when one changes from the divalent to the trivalent matrix.

ACKNOWLEDGMENT

We would like to thank A. J. Freeman for helpful discussions.

*Work at Argonne National Laboratory performed under the auspices of the U.S. Atomic Energy Commission.

†Present address: Hebrew University, Jerusalem, Israel.

[1]S. Hufner and J. H. Wernick, Phys. Rev. **173**, 448 (1968).

[2]H. Zmora, M. Blau, and S. Ofer, Phys. Lett. A **28**, 668 (1969).

[3]J. H. Wernick, H. J. Williams, and A. C. Gossard, J. Phys. Chem. Solids **28**, 271 (1966).

[4]R. C. Sherwood, H. J. Williams, and J. H. Wernick, J. Appl. Phys. **35**, 1049 (1964).

[5]H. H. Wickman, I. Nowik, J. H. Wernick, D. A. Shirley, and R. B. Frankel, Phys. Rev. **37**, 1246 (1966).

[6]F. Dintelmann and K. H. J. Buschow, Z. Angew. Phys. **31**, 181 (1971).

PHYSICAL REVIEW B VOLUME 8, NUMBER 1 1 JULY 1973

Dynamic Spin Configuration for Hard Magnetic Bubbles in Translational Motion

A. A. Thiele, F. B. Hagedorn, and G. P. Vella-Coleiro
Bell Laboratories, Murray Hill, New Jersey 07974
(Received 29 November 1972)

The detailed model of Vella-Coleiro *et al.* for steady translational motion of a hard bubble (i.e., a cylindrical magnetic domain with axial Bloch lines distributed nonuniformly around the domain wall) is shown to lead to essentially the same results obtained by Slonczewski and to exacly the same results obtained by Thiele in less specific calculations. These theoretical expressions are shown to give a good description of new experimental observations of hard-bubble dynamics.

Several theories have been reported[1–4] recently for the dynamic behavior of hard-magnetic-bubble domains (i.e., cylindrical domains whose walls contain axial Bloch lines). Steady translational motion is considered in Refs. 1, 3, and 4, while bubble-collapse dynamics is the subject of Ref. 2. Substantially different conclusions are presented in Ref. 1 than in Refs. 3 and 4. The purpose of the present paper is to show that the basic model used to develop the nonlinear theory of Ref. 1 can yield

essentially the same results as those given in Refs. 3 and 4 and that we can calculate the magnitude of the drive-field-dependent function f which was determined only from experimental data in Ref. 1. We then show that these expressions, when modified to account for coercivity, provide a good description of extensive new experimental results.

We start by writing the Gilbert equation in the form[5]

$$\dot{\theta}=\frac{\gamma}{M}\frac{\delta E}{\delta\phi}-\alpha\dot{\phi}\sin\theta\ , \tag{1a}$$

$$\dot{\phi}\sin\theta=\frac{\gamma}{M}\frac{\delta E}{\delta\theta}+\alpha\dot{\theta}\ , \tag{1b}$$

where θ and ϕ are the polar angles of the magnetization vector $\vec{M}$, α is the phenomenological damping constant, and γ is the magnitude (i.e., $\gamma>0$) of the electronic gyromagnetic ratio. The factors $\delta E/\delta\phi$ and $\delta E/\delta\theta$ will be discussed below. For the sake of simplicity we will consider the cylindrical wall to be represented by an array of planar wall segments. Consequently, we assume θ and ϕ to depend only on the Cartesian coordinates x and y, where x is in the direction normal to the plane of the planar domain wall. As was done in Ref. 1, we focus our attention on the center of the wall (where $\theta=\frac{1}{2}\pi$) and make the following assumptions:

$$\dot{\theta}=v_x\frac{\partial\theta}{\partial x}\ ,\qquad \dot{\phi}=v_y\frac{\partial\phi}{\partial y}\ ,\qquad \frac{\partial\theta}{\partial x}=\frac{\pi}{l_w}\ . \tag{2}$$

In (2), l_w is the wall width, and the steady-velocity components of the moving wall are v_x and v_y. Substituting (2) into (1) yields

$$\frac{\pi v_x}{l_w}=\frac{\gamma}{M}\frac{\delta E}{\delta\phi}-\alpha v_y\frac{\partial\phi}{\partial y}\ , \tag{3a}$$

$$v_y\frac{\partial\phi}{\partial y}=\frac{\gamma}{M}\frac{\delta E}{\delta\theta}+\frac{\alpha\pi v_x}{l_w}\ . \tag{3b}$$

The terms in (3) have a one-to-one correspondence[6] with those of the general planar wall response function. Therefore, these equations can be applied to a cylindrical wall configuration of the type suggested in Ref. 1.

Figure 1 shows the assumed domain configuration, both in the static and dynamic states. The bubble-domain diameter is d, and the total number of Bloch line *pairs* is n. Consequently, $\partial\phi/\partial y=2n/d$ in the static case, since we consider only the case for large n where this approximation has been shown[7] to be reasonable. For the dynamic case we postulate the distribution of the Bloch lines according to

$$\frac{\partial\phi}{\partial y}=\frac{2n}{d}\left(1+\frac{v}{v_m}\cos\xi\right), \tag{4}$$

where $v^2=v_x^2+v_y^2$ and v_m is a parameter to be evaluated. Note that (4) is equivalent to Eq. (10) of Ref. 1, although for simplicity we consider only one sign for the sense of rotation within the Bloch line.

We are now in a position to evaluate the $\delta E/\delta\phi$ and $\delta E/\delta\theta$, which are the functional derivatives with respect to ϕ and θ of the magnetic-free-energy density of the system under consideration. In order to simplify the problem, we assume that the bubble domain shape is not changed in any significant way by the translational motion and that most of the terms in these derivatives cancel out in the dynamic case just as they do in the static case.

As was noted in Ref. 1, the only significant term which remains in $\delta E/\delta\phi$ is $2A(\partial^2\phi/\partial y^2)$, where A is the exchange constant. However, two significant terms remain in $\delta E/\delta\theta$. Reference 1 shows one term to be $-MH_0\sin(\xi-\xi_f)$, which corresponds to the external-field gradient that makes the bubble domain move. The other term arises from the variation in the wall energy around the domain perimeter, which is implied by (4). In the theory[8] of bubble-domain stability, it is shown that the wall energy σ_w leads to an effective field which tends to collapse the bubble domain. Equation (4) modulates this field around the perimeter. The general results that $\pi/l_w\rightarrow\partial\phi/\partial y$ for large n (Refs. 6 and 9) and $\sigma_w l_w=4\pi A$ (Ref. 6) enable writing the wall energy in the limit of large n as $\sigma_w=4A(\partial\phi/\partial y)$. Since σ_w is only a function of $\partial\phi/\partial y$, the variational process denoted by $\delta E/\delta\theta$ operates only on the factor representing the wall area, and the wall energy appears in the effective-field expression exactly in the conventional[8] way: σ_w/d. By using (4) for $\partial\phi/\partial y$, the variable term in the effective wall-energy field is thus seen to be $(8nAv/d^2v_m)\cos\xi$.

We now postulate that the steady-state motion of the bubble domain is along a direction such that the velocity components for the segment of the domain wall at angle ξ (see Fig. 1) are

$$v_x=v\sin(\xi-\xi_0),\qquad v_y=v\cos(\xi-\xi_0)\ . \tag{5}$$

Substituting the above expressions for v_x, v_y, $\delta E/\delta\phi$, $\delta E/\delta\theta$, l_w, and $\partial\phi/\partial y$ into (3) results in

$$v[1+(v/v_m)\cos\xi][\sin(\xi-\xi_0)+\alpha\cos(\xi-\xi_0)]=(-4\gamma Av/Mdv_m)\sin\xi \tag{6a}$$

and

$$v[1+(v/v_m)\cos\xi][\cos(\xi-\xi_0)-\alpha\sin(\xi-\xi_0)]=(-\gamma dH_0/2n)\sin(\xi-\xi_f)+(4\gamma Av/Mdv_m)\cos\xi\ . \tag{6b}$$

At this point, we must determine if values can be found for the parameters ξ_0, ξ_f, v, and v_m which satisfy (6) for any value of ξ. By neglecting v^2 terms in (6), these parameters can be shown to be

$$\xi_0=\tan^{-1}\alpha, \tag{7a}$$

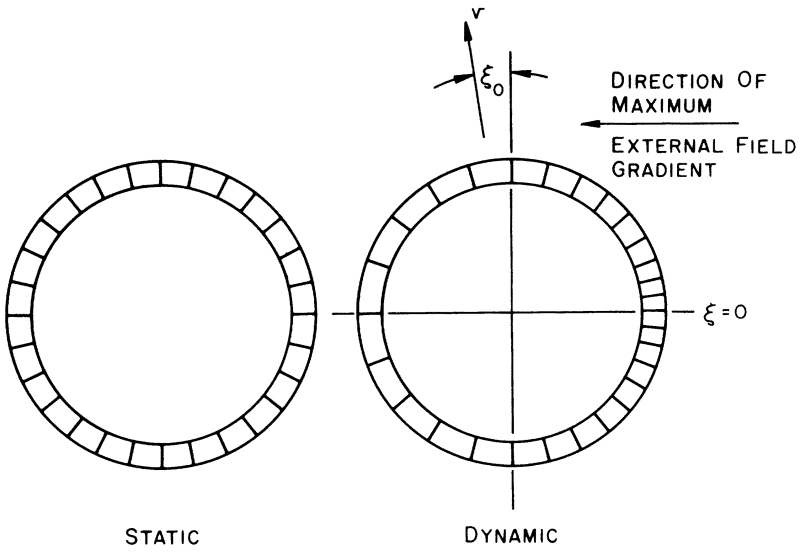

FIG. 1. Schematic representation of the Bloch line distribution in static and dynamic hard-bubble domains. The radial bars indicate the locations of the Bloch line centers. The field gradient is drawn for $\xi_f = -\frac{1}{2}\pi$.

$$v_m = -4\gamma A/[Md(1+\alpha^2)^{1/2}]\,, \tag{7b}$$

$$\xi_f = \pm\tfrac{1}{2}\pi, \tag{7c}$$

$$v = \pm\gamma d H_0/[4n(1+\alpha^2)^{1/2}]\,. \tag{7d}$$

Comparing (4), (7b), and (7d) with Eq. (10) of Ref. 1 evaluates the f function of that paper, although it should be noted that the spin distribution in Fig. 1 is rotated by ~ 90° with respect to that shown in Fig. 2 of Ref. 1. We find $f = \frac{1}{2}\alpha$ for our linearized solution. If this value is substituted into Eq. (15) of Ref. 1, their ratio of the velocity components perpendicular and parallel to the direction of maximum field gradient becomes $\mp\sqrt{2}\,(\alpha+\frac{1}{2})/(1-\frac{1}{2}\alpha)$. From (7) and Fig. 1, it is apparent that our value for this ratio is quite different and is $\cot\xi_0 = 1/\alpha$, an expression which agrees exactly with Eq. (13) of Ref. 3 in the absence of coercivity and Eq. (25b) of Ref. 4. Moreover, it may be seen that our Eq. (7d) is equivalent to Eq. (25a) of Ref. 4.

An additional comparison can be made with Ref. 3. The quantities V, $V_\perp$, and H_a in Ref. 3 are denoted in the present paper as v, $v\cos\xi_0$, and $2H_0$. Consequently, our results show that

$$2V^2/\gamma d V_\perp = H_a/4n\,, \tag{8}$$

which differs from Slonczewski's Eq. (12) by a factor of 4. However, there is a factor of 2 difference in the definition of n. It also appears that Slonczewski has not considered the variation of $\partial\phi/\partial y$ around the perimeter of the bubble, which exactly accounts for a second factor of 2 in our calculation. While footnote 10 of Ref. 3 indicates that a more rigorous calculation introduces a correction factor of 2, it should be borne in mind that Slonczewski uses a constant-twist expression in deriving Eq. (8) of Ref. 3. Use of a constant-twist expression here, rather than (4), would make it impossible to find a nontrivial solution for (3a).

Modification of (7) to include coercivity is required in order to compare our results with experiment. Our approach is *ad hoc* and is similar to that followed by Slonczewski.[3] Subsequently, we use the notation $H_a \equiv 2H_0$ to define the product of the maximum field gradient with the bubble diameter. From (7) and Fig. 1, it may be seen that the components of H_a parallel and perpendicular to the direction of the bubble domain velocity are

$$H_\parallel = H_a \sin\xi_0 = \pm 8nv\alpha/\gamma d \tag{9a}$$

and

$$H_\perp = H_a \cos\xi_0 = \pm 8nv/\gamma d\,. \tag{9b}$$

We now postulate that the domain coercivity H_{cd} is added to $H_\parallel$ and that the vectorial sum of $H_\parallel + H_{cd}$ and $H_\perp$ be just equal to the applied field:

$$(\pm 8n\alpha v/\gamma d + H_{cd})^2 + (\pm 8nv/\gamma d)^2 = H_a^2\,. \tag{10a}$$

If we define a velocity v_c to be

$$v_c \equiv \gamma d H_{cd}/8n\,, \tag{10b}$$

then we see the angle between the velocity direction and the direction of maximum field gradient is $\frac{1}{2}\pi - \xi_{oc}$, as in Fig. 1, where

$$\tan\xi_{oc} \equiv (H_\parallel + H_{cd})/H_\perp = \alpha + v_c/|v|\,. \tag{10c}$$

Plotting measured values of $\tan\xi_{oc}$ as a function of $1/|v|$ therefore yields a straight line whose slope is v_c and whose intercept is α. These values are useful to calculate a quantity V_n, which is obtained after rearranging (10a):

$$V_n \equiv [(1+\alpha^2)(v/v_c)^2 + 2\alpha|v|/v_c + 1]^{1/2} = H_a/H_{cd}\,. \tag{10d}$$

A plot of V_n as a function of H_a is thus expected to be a straight line through the origin with inverse slope H_{cd}. Direct measurement of the bubble diameter gives d, so that values of v_c and H_{cd} determined from the slopes yield n from 10(b).

New hard-bubble dynamic measurements have been made with an epixtaxial film of $Y_1Gd_1Tm_1Ga_{0.8}Fe_{4.2}O_{12}$. Two different hard bubbles, 4.5 and 5.8 μm in diameter, were used, and these measurements are plotted according to (10c) and (10d) in Figs. 2 and 3, respectively. It is seen that the plots are well described by straight lines in all cases. The parameters extracted from the plots are (for the 4.5- and 5.8-μm bubbles, respectively) $\alpha = 0.014$, 0.040; $H_{cd} = 0.73$, 0.67 Oe; $n = 52$, 57. Preliminary data, obtained from Ref. 1, were plotted in a similar fashion previously in Ref. 3.

These values for n are typical of values reported[7] for static measurements of hard bubbles in this material, and values from 0.9 to 1.0 Oe are measured for the minimum H_a required for bubble motion. Although these values of α are lower by about a factor of 10 than the damping constant extracted from the normal bubble-domain wall mobility, measurements of the resonance linewidth[10] at 13.15 GHz on two different samples of these epitaxial films have given values for the Gilbert damping constant of 0.03 and 0.04. While there appears to be some uncertainty as to the exact interpretation that should be placed on the value of the intercepts on the plots in Fig. 2, a surprisingly good description of these dynamic hard-bubble measurements would be provided by (10b)–(10d) by making only minor fitting adjustments to the parameters obtained from resonance linewidth and other independent measurements.

Two final comments are of interest. First, the values for the damping parameter ($\alpha = 0.014$ and $\alpha = 0.040$) which were obtained from the data shown in Fig. 2 resulted from a least-squares fitting of these data to (10c). However, only a minor adjustment of the slopes of the two lines shown in Fig. 2 would lead to a common value for the extrapolated intercepts, and these data certainly cannot be taken as unambiguous proof that α was definitely different for the two bubble domains in the same material.

The second comment concerns the fact that Eqs. (7) were obtained by neglecting v/v_m with respect

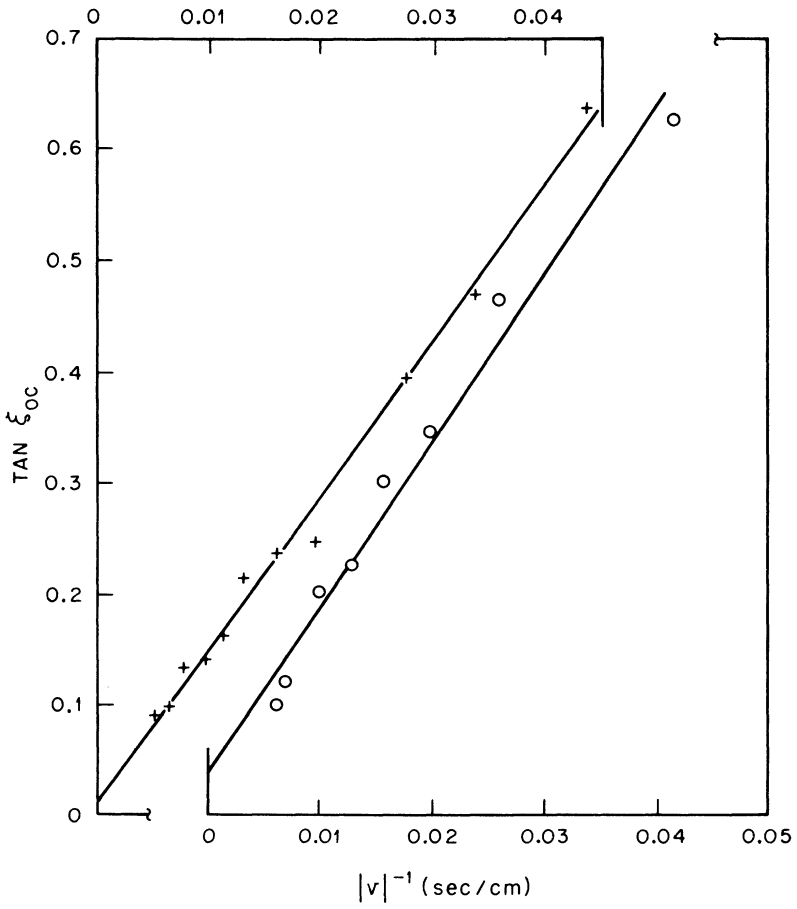

FIG. 2. Plot of experimental hard-bubble measurements according to Eq. (10c): + and O for the 4.5- and 5.8-μm bubbles, respectively.

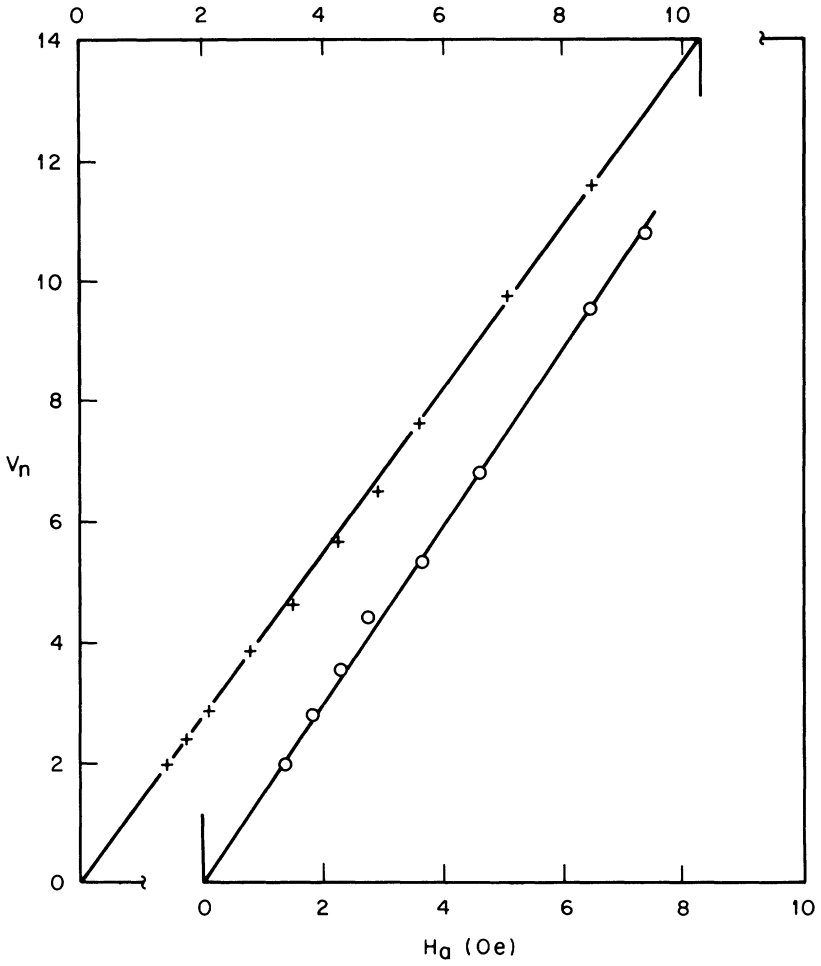

FIG. 3. Plot of experimental hard-bubble measurements according to Eq. (10d); + and O for the 4.5- and 5.8-μm bubbles, respectively.

to unity. For the data shown in Figs. 2 and 3 and in Ref. 1, $v/v_m \leq 0.1$. Consequently, a higher-order solution would be of some interest, particularly for the larger velocities. In this context, we note that an exact solution of (6) would result from (7) if we had taken

$$\frac{\partial\phi}{\partial y} = \frac{2n}{d} \exp\left(\frac{v}{v_m}\cos\xi\right) \tag{11a}$$

and

$$H_g = \tfrac{1}{2}(H_0\cos\xi)\{[1 + v_m/v\cos\xi] \times \exp[(v/v_m)\cos\xi] - v_m/v\cos\xi\}\ , \tag{11b}$$

where H_g is the field gradient. [Note that expanding (11) and keeping only the first-order terms in $\cos\xi$ leads to the expressions used originally for $\partial\phi/\partial y$ and H_g.] However, (6) would still not be exact, since approximations were made in evaluating $\delta E/\delta\phi$, $\delta E/\delta\theta$, and l_w. The validity of these approximations, particularly with regard to higher-order terms in v/v_m, has not been determined.

The authors thank W. J. Tabor for useful discussions during the course of this work and R. C. LeCraw for permission to quote his unpublished work.

[1]G. P. Vella-Coleiro, A. Rosencwaig, and W. J. Tabor, Phys. Rev. Lett. **29**, 949 (1972).
[2]A. P. Malozemoff and J. C. Slonczewski, Phys. Rev. Lett. **29**, 952 (1972).
[3]J. C. Slonczewski, Phys. Rev. Lett. **29**, 1679 (1972).
[4]A. A. Thiele, Phys. Rev. Lett. **30**, 230 (1973).
[5]J. C. Slonczewski, Int. J. Magn. **2**, 85 (1972).
[6]A. A. Thiele (unpublished).
[7]A. Rosencwaig, W. J. Tabor, and T. J. Nelson, Phys. Rev. Lett. **29**, 946 (1972).
[8]A. A. Thiele, Bell Syst. Tech. J. **48**, 3287 (1969).
[9]See Eq. (11) of Ref. 3, for example.
[10]R. C. LeCraw (private communication).